On The Asynchronously Continuous Control of Mobile Robot Movement By Motor Cortical Spiking Activity

Zhiming Xu, Rosa Q. So, Kyaw Kyar Toe, Kai Keng Ang and Cuntai Guan

***Abstract*— This paper presents an asynchronously intracortical brain-computer interface (BCI) which allows the subject to continuously drive a mobile robot. This system has a great implication for disabled patients to move around. By carefully designing a multiclass support vector machine (SVM), the subject's self-paced instantaneous movement intents are continuously decoded to control the mobile robot. In particular, we studied the stability of the neural representation of the movement directions. Experimental results on the nonhuman primate showed that the overt movement directions were stably represented in ensemble of recorded units, and our SVM classifier could successfully decode such movements continuously along the desired movement path. However, the neural representation of the stop state for the self-paced control was not stably represented and could drift.**

***Index Terms*— Brain-computer interface, maximal a posterior, motor cortex, neural decoding, support vector machine.**

I. Introduction

Brain-computer interface (BCI) directly reads the neural signals from the brain and translates them as commands to an external device to help the disabled patients who have a broken neural pathway from brain to limbs [1], [2]. One of the core parts in BCI is the neural signal processing which provides such translation. During the last decade, several groups have demonstrated the capability of extracting cortical neuronal activity from motor areas of brain for controlling computer cursor or robotic arm through experiments on both non-human primates [3]–[8] and humans patients [9], [10]. These experiments showed great promise of BCI for the help of patients with broken neural pathway. However all these demonstrations required the subjects sit still in a chair during controlling external devices.

In this work, we built a brain-controlled mobile robot which allows a subject himself to drive the mobile robot in a two dimensional planar space. We employed asynchronous (self-paced) BCI to control the mobile robot using a novel feedback to the subject. This is more realistic to the real world scenario where a disabled patient sits on a wheelchair. The issue arises on how the feedback would influence the cortical neuronal activity which serves as the source of control commands. The previous work showed the motor cortex can form a stable cortical map [11] when the subject sat still to control computer cursor. Similarly we studied whether or not a stable cortical representation of movement parameters like directions can be formed under the movement feedback and tested it within the closed-loop online control. This paper presents our initial finding to study the neural representation of the different movement directions and the stop state used in our continuous control.

*This work was supported by the Science and Engineering Research Council of Agency for Science, Technology and Research (ASTAR).

Z. Xu, R.Q. So, K.K. Toe, K.K. Ang and C. Guan are with the Department of Neural and Biomedical Technology, Institute for Infocomm Research, ASTAR Singapore, 138632 (email: {xuz, rosa-so, kktoe, kkang, ctguan}@i2r.a-star.edu.sg)

II. Materials and Methods

All procedures and experiments described here were approved by the Institutional Animal Care and Use Committee of ASTAR and conformed to the Guidelines for the Care and Use of Laboratory Animals.

A. Behavior Task

One male rhesus macaque was seated in a primate chair which was put on top of the mobile robot while his forearm was abducted 90 degree and supported by the primate chair. The monkey was trained to use a joystick to perform three movement directions (right, forward, left) in two-dimensional space from his wrist movement to drive a mobile robot moving with constant speed. In addition, the monkey also learned to stop the movement by holding the joystick at the origin position. The stop state is the fourth brain state in addition to the three directional movements. This is different from the previous computer cursor tasks [4]–[7] where the feedback about the movement was immediately available and shown on the computer screen. In this case, the feedback of self-movement along with the mobile robot was considerably delayed due to the physically limited acceleration time of the motor engine of the mobile robot. Our behavioral task is similar to the pursuit tracking task [12] where the monkey was triggered to track a visual target (the monkey trainer) by operant conditioning. At the start of each trial, a monkey trainer visually cued the monkey where to move by using a liquid reward and the monkey was allowed to move on his own pace (asynchronously) by continuously control the joystick to reach the target to get the reward. After successfully acquiring the target, the monkey trainer moved randomly to a new place in the working space ($\sim 6 \times 4\ m^2$) and the monkey was cued to move accordingly.

B. Neural and Kinematics Recordings

Four floating microelectrode arrays (MicroProbes, Gaithersburg, MD, United States) were implanted anterior to the central sulcus in the arm area of the contralateral primary motor cortex (MI) to the trained (right) arm. Total 96 single-electrode were available (two arrays of 32 electrodes and two arrays of 16 electrodes) with tip impedance of ~ 0.5 MΩ. Neuronal spiking activity from all arrays were simultaneously recorded with a Plexon data

978-1-4244-7929-0/14/$26.00 ©2014 IEEE

acquisition system (Plexon Inc. Texas, TX, United States) during each experimental session. Spike waveforms were sampled at 40kHz. Spike sorting was performed manually at the beginning (a few minutes) of neural recording using manually set threshold and spike waveform matching by Plexon online sorter and fixed thereafter in each day. Normally between 30 and 40 units (including possible multiunits) can be identified and recorded. Units averaged firing rate below 1Hz were discarded for further analysis.

Simultaneously with neural recordings, analog joystick signals (two channels for x- and y-axis) accompanying the overt wrist movement were also recorded from Plexon system by using external analog input channels and synchronized with neural recordings. After manual calibration on these joystick signals, we further define the four different classes representing right/left/forward movement and stop with an appropriate voltage range. During offline processing and neural decoder construction, the four different classes were extracted along each session by the joystick signals and the corresponding neuronal spiking activity were segmented as inputs for the decoder.

C. Classifier Design

We employed the support vector machine (SVM) to classify the neuronal spike data. SVM uses a hyperplane f to separate different classes of input data $\mathbf{x}$ in a feature space ϕ induced by the chosen kernel function K, [13], [14]

$$f(\mathbf{x}) = \mathbf{w}^T \phi(\mathbf{x}) + b \tag{1}$$

where $\mathbf{w}$ and b are the normal vector and intercept of the hyperplane, respectively. The binary classification was done by checking sign(f) for two different classes, i.e., $f(\mathbf{x}) > 0$ for the decision of $\mathbf{x}$ belonging to one class and $f(\mathbf{x}) < 0$ otherwise. The hyperplane f optimized by SVM is the one that maximizes the margin which is defined as the distance from the nearest training samples to the hyperplane. Maximizing the margin is known to increase the generalization capacity [13], [14]. In addition, one advantage of SVM is its robustness to outliers by carefully searching support vectors and using regularization to minimize the effects of outliers. These outliers usually greatly distort the decision boundary of the conventional linear classifier [14].

Classical SVM only deals with binary classification and it was necessary to extend to multiclass scenario for this study. A popular strategy is to reduce the multiclass problem into multiple binary classification problems and then combined the outputs from each binary classifiers [15], including one-vs-all and one-vs-one approaches. However, these conventional strategies only used each binary classification decision to yield the decision for the multiclass decision using some rule like majority voting and thus completely overlooked the estimated posterior class probabilities. As pointed in [16], conventional methods can be improved by pairwise coupling those estimated probabilities. In this work, we adopted the LIBSVM software for implementing the binary SVMs [17] and used the sigmoid function [18] for estimating the binary class posterior probability $p^b_{i,kl}$ of classes k-vs-l for the training dataset $\{\mathbf{x}_i, y_i\}$,

$$\begin{aligned} p^b_{i,kl} &= Pr(y_{i,k} = 1 | \mathbf{x}_i, y_{i,k} = 1 \text{ or } y_{i,l} = 1) \\ &= 1/(1 + \exp(A_{kl} f_{i,kl} + B_{kl})) \end{aligned} \tag{2}$$

where $f_i = \mathbf{w}^T_{kl}\phi(\mathbf{x}_i) + b_{kl}$ is the signed margin of a binary SVM. The parameters A_{kl} and B_{kl} can be learned logistic regression using Newton's method with backtracking [19]. Furthermore, we employed the improved pairwise coupling for estimating the multiclass probabilities $P^m_{i,k}(k = 1, \cdots, M)$ from all pairwise $p^b_{i,kl}$ for input data $\mathbf{x}_i$ [20]. The final classification decision $\hat{y}_i$ for the data sample $\mathbf{x}_i$ is based on the maximal a posterior probability over all M classes.

$$\hat{y}_i = \arg \max_{1 \le k \le M} P^m_{i,k} \tag{3}$$

Both linear $\left(K_l(\mathbf{x}, \mathbf{y}) = \mathbf{x}^T\mathbf{y}\right)$ and Gaussian $\left(K_g(\mathbf{x}, \mathbf{y}) = \exp(-\gamma\|\mathbf{x} - \mathbf{y}\|^2)\right)$ kernels were tested, and we only reported the results of the linear kernel in this paper (results of Gaussian kernel are similar). The classifier performance only depended on the single tuning parameter C, i.e., the regularizer, and we employed 5-fold cross-validation to optimize it using only the training data.

III. Results and Discussion

We have applied our designed classifier presented in Sec. II-C to the neuronal data recorded *in vivo* from a rhesus monkey performing the pursuit tracking task presented in Sec. II-A. The input vector $\mathbf{x}$ to the SVM classifier was the spike counts of the online sorted units calculated in a time bin of $\Delta t = 500$ ms. For continuous control, the classifier was operated in 10 Hz (i.e., every 100 ms) on the time bin just before that time instant. Thus the time bin overlapped 400 ms in time with adjacent time bin for a smooth continuous control. Here, we reported the results of two different days of experiments across two weeks. On each day, the monkey first used his right hand to control the joystick to drive the mobile robot (i.e., hand control) and the corresponding recorded data was chosen for training SVM (i.e., training session). After training, the control of the mobile robot was taken over by the trained SVM (i.e., brain control), while the monkey was still allowed to use his hand to move the joystick but the joystick signal was disconnected from the mobile robot. In this way, it was easy to cue the monkey to do the task and to keep his attention. Under brain control, the joystick signal was still recorded to provide the monkey's intended movement when evaluating the performance of our classifier (i.e., test session). The number of training samples ($n = 1400$) was kept fixed for both days and evenly distributed in all four classes by random resampling. However, the number of test samples (separate from training) is usually different from each day depending on the test session. We adopted the correct estimation accuracy, kappa coefficient and the confusion matrix as the performance measure for our classifier, as suggested and commonly used in BCI [21].

A. Classification performance

Fig. 1 shows the visualization of neural representation of movements for both training (left panel) and test (right panel) sessions of one data set, in terms of a low dimensional space

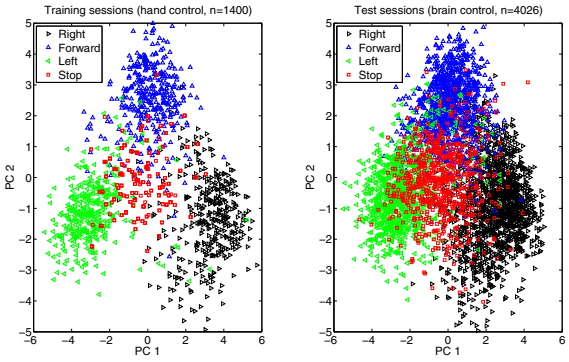

Fig. 1. The first two principle component projections of SVM signed distances of spike count vectors for our define four classes of movements. Analysis was performed on data set C20140211.

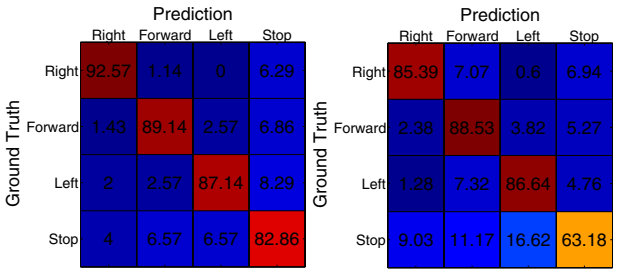

(a) Training. (b) Test.

Fig. 2. Comparison of the confusion matrices of both training and test sessions from data set C20140211.

which was defined during the training session by the first two principle components of the signed distance vector $\mathbf{f}_i$ of each spike count vector $\mathbf{x}_i$ where the vector $\mathbf{f}_i$ was composed of all pairwise binary SVM (6 binary SVMs for four classes). In this projection space, it can be seen clearly the colored points for each class of data clustered into groups corresponding to the our defined movement states. In particular, the clusters for the three movement directions stay relatively more stable than the state of stop which tends to disperse more when changed from hand control session to brain control session. In addition, the confusion matrices were visualized in Fig. 2 for both training and test sessions of the same data set as shown in Fig. 1. The total classification accuracy and the kappa coefficient ($\pm$ standard error) for the training session are 87.93% and $0.839(\pm 0.032)$, respectively, whereas they are 82.56% and $0.762(\pm 0.019)$, respectively, for the test session. It can be seen clearly the performance drop of the stop state compared to the others due to the its spread and thus overlap with others.

B. Nonstationary brain state of 'stop'

We show the result for a later day experiment (one week after the previous one) in Fig. 3 using the same way of visualization as shown in Sec. III-A. Although the features in the projection space is similar to that of Fig. 3 during the

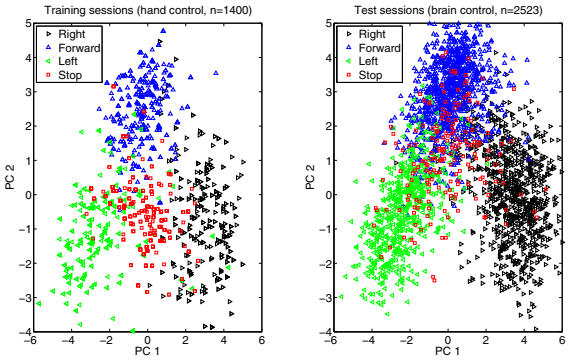

Fig. 3. Same way of visualization as in Fig. 1. Analysis was performed on data set C20140219

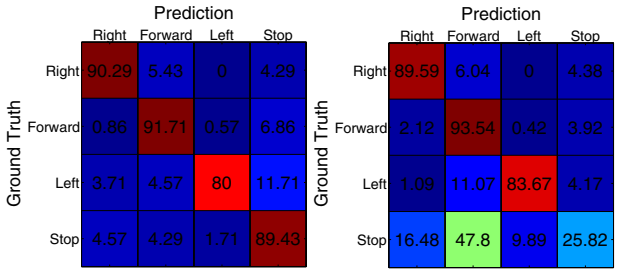

(a) Training. (b) Test.

Fig. 4. Comparison of the confusion matrices of both training and test sessions from data set C20140219.

training session, it can be seen clearly the difference of the state of stop between these two days of recordings. Other than only spread in Fig. 1, the features of stop state also showed *drift* between training and test sessions. Such drift resulted in the classification performance drop during the test session for the stop state as shown in Fig. 4(b) when compared to the training session shown in Fig. 4(a). Such performance drop yielded increased false positive for the detection between intending to move and staying stopped. Other than the drift of the stop state, the other three classes of movements showed relatively stationary feature distributions and thus relatively stable classification performance came along with. The overall classification accuracy and the kappa coefficient for the training session are 87.86% and $0.838(\pm 0.032)$, respectively, whereas they are 85.18% and $0.784(\pm 0.025)$, respectively, for the test session. Although the overall performance looked similar, the behavior of the monkey changed to combat the misclassification of the stop state. For example, when he was trying to stop to acquire the juice reward during brain control and the classifier issued a wrong decision of turning right, he would try to correct the error by counter turning to the other direction (i.e., left).

C. Discussion

It was reported [22] the possible intra-day signal instability in terms of changes in unit firing rate and spike waveform

amplitude and suggested most of the rate changes likely emerged from neurophysiological mechanisms. In particular, they have found some directional bias in the decoded cursor movements, which were consistent with the pioneering works [4], [6]. This may explain the possibly nonstationary stop state of our data. In contrast, the relatively stable representation of three movement directions were consistent with the existing works using spikes [23] and MEG [24]. They have also shown similar representation of movement directions in different low dimensional spaces. These works altogether suggested the neuronal spikes are more correlated with movement kinematics than the cognitive states of brain, which was clearly reflected in terms of neural representation and class-specific classification accuracy as presented in Sec. III-B. What characteristics of the cognitive state of brain for stop in terms of neuronal spikes is still an open question.

Such nonstationarity of neural signals was also discussed in [25] for EEG-based BCI. In addition, it was reported [26] that the local field potential (LFP) spectrum and amplitude changes were well time-locked to the movement onset in self-paced reaches. A recent work [27] further compared the spike-based and LFP-based state decoder and showed the superior performance of LFP for the state transition into the reaction and movement. These works suggested field potentials, especially LFP, might correlate better with the cognitive state of brain than the neuronal spikes. How to efficiently integrate the LFP for more reliably decoding the stop state is an issue to address in our future work.

IV. Conclusion

This work showed the monkey can operate our asynchronous BCI to continuously drive a mobile robot through closed-loop online experiments, which has great implication for disabled patients. We have shown the neuronal representation of the movement directions is stable across one week, and our SVM classifier can successfully decode such movements for continuous control along the desired movement trajectory. However, the representation of the stop state could drift even across sessions of one day, which could decrease the efficiency of the system. This posed the challenge for stable and efficient asynchronous control using brain signals. It remains to be understood the neurophysiological mechanism and representation of the stop state in terms of either LFP or spiking activity. This study presented our initial attempt to study the stop state of brain using spikes within the context of BCI. Further investigations have to be done on tracking and adaptation of the nonstationarity of the stop state in either LFP or spiking activity, and on how to successfully incorporate into the BCI framework.

Acknowledgements

We thank Dr. Camilo Libedinsky and Prof. Shih-Cheng Yen for valuable discussions, and Mr. Duncun, Mr. Clement and Ms. Rev for training monkeys and veterinary care.

References

[1] J. P. Donoghue, "Bridging the brain to the world: a perspective on neural interface systems," *Neuron*, vol. 60, pp. 511 – 521, 2008.

[2] M. A. L. Nicolelis and M. A. Lebedev, "Principles of neural ensemble physiology underlying the operation of brain-machine interfaces," *Nature Review Neurosci.*, vol. 10, pp. 530 – 540, 2009.

[3] A. P. Georgopoulos, R. E. Kettner, and A. B. Schwartz, "Primate motor cortex and free arm movements to visual targets in three-dimensional space. II. coding of the direction of movement by a neuronal population," *J. Neurosci.*, vol. 8, pp. 2928 – 2937, 1988.

[4] D. M. Taylor, S. I. Tillery, and A. B. Schwartz, "Direct cortical control of 3D neuroprosthetic devices," *Science*, vol. 296, pp. 1829 – 832, 2002.

[5] M. D. Serruya, N. G. Hatsopoulos, L. Paninski, M. R. Fellows, and J. P. Donoghue, "Instant neural control of a movement signal," *Nature*, vol. 416, pp. 141 – 142, 2002.

[6] J. M. Carmena *et al*., "Learning to control a brain-machine interface for reaching and grasping by primates," *PLoS Biol.*, vol. 1, pp. 193 – 208, 2003.

[7] G. Santhanam *et al*., "A high-performance brain-computer interface," *Nature*, vol. 442, pp. 195 – 198, 2006.

[8] M. Velliste *et al*., "Cortical control of a prosthetic arm for self-feeding," *Nature*, vol. 453, pp. 1098 – 1101, 2008.

[9] W. Truccolo, G. M. Friehs, J. P. Donoghue, and L. R. Hochberg, "Primary motor cortex tuning to intended movement kinematics in humans with tetraplegia," *J. Neurosci.*, vol. 28, pp. 1163 – 1178, 2008.

[10] L. R. Hochberg *et al*., "Reach and grasp by people with tetraplegia using a neurally controlled robotic arm," *Nature*, vol. 485, pp. 372 – 377, 2012.

[11] K. Ganguly and J. M. Carmena, "Emergence of a stable cortical map for neuroprosthetic control," *PLoS Biol.*, vol. 7, pp. 1 – 13, 2009.

[12] L. Paninski, M. R. Fellows, N. G. Hatsopoulos and J. P. Donoghue, "Spatiotemporal tuning of motor cortical neurons for hand position and velocity," *J. Neurophysiol.*, vol. 91, pp. 515 – 532, 2004.

[13] C. J. C. Burges, "A tutorial on support vector machines for pattern recognition," *Knowledge Discovery and Data Mining*, vol. 2, pp. 121 – 167, 1998.

[14] C. M. Bishop, *Pattern Recognition and Machine Learning*. Springer, 2006.

[15] E. L. Allwein, R. E. Schapire and Y. Singer, "Reducing multiclass to binary: a unifying approach for margin classifiers," *J. Machine Learning Research*, vol. 1, pp. 113 – 141, 2000.

[16] T. Hastie and R. Tibshirani, "Classification by pairwise coupling," *The Annals of Statistics*, vol. 26, pp. 451 – 471, 1998.

[17] C.-C. Chang and C.-J. Lin, "LIBSVM: A library for support vector machines," *ACM Transactions on Intelligent Systems and Technology*, vol. 2, pp. 27:1–27:27, 2011, software available at http://www.csie.ntu.edu.tw/∼cjlin/libsvm.

[18] J. Platt, "Probabilistic outputs for support vector machines and comparison to regularized likelihood methods," in *Advances in Large Margin Classifiers*, A. Smola *et al.*, Ed. MIT Press, 2000.

[19] H.-T. Lin, C.-J. Lin and R. C. Weng, "A note on Platt's probabilistic outputs for support vector machines," *Mach. Learn.*, vol. 68, pp. 267 – 276, 2007.

[20] T.-F. Wu, C.-J. Lin and R. C. Weng, "Probability estimates for multi-class classification by pairwise coupling," *J. Machine Learning Research*, vol. 5, pp. 975 – 1005, 2004.

[21] A. Schlögl, J. Kronegg, J. E. Huggins and S. G. Mason, "Evaluation criteria for BCI research," in *Toward Brain-computer Interfacing*, G. Dornhege *et al.*, Ed. MIT Press, 2007.

[22] J. A. Perge *et al.*, "Intra-day signal instabilities affect decoding performance in an intracortical neural interface system," *J. Neural Eng.*, vol. 10, pp. 1 – 14, 2013.

[23] G. Santhanam *et al.*, "Factor-analysis methods for higher-performance neural prostheses," *J. Neurophysiol.*, vol. 102, pp. 1315 – 1330, 2009.

[24] W. Wang *et al.*, "Decoding and cortical source localization for intended movement direction with MEG," *J. Neurophysiol.*, vol. 104, pp. 2451 – 2461, 2010.

[25] P. Shenoy, M. Krauledat, B. Blankertz, R. P. N. Rao and K.-R. Müller, "Towards adaptive classification for BCI," *J. Neural Eng.*, vol. 3, pp. 13 – 23, 2006.

[26] E. J. Hwang and R. A. Andersen, "Brain control of movement execution onset using local field potentials in posterior parietal cortex," *J. Neurosci.*, vol. 29, pp. 14 363 – 14 370, 2009.

[27] V. Aggarwal, M. Mollazadeh, A. G. Davidson, M. H. Schieber and N. V. Thakor, "State-based decoding of hand and finger kinematics using neuronal ensemble and LFP activity during dexterous reach-to-grasp movements," *J. Neurophysiol.*, vol. 109, pp. 3067 – 3081, 2013.